Received: Added at production | Revised: Added at production | Accepted: Added at production

DOI: xxx/xxxx

RESEARCH ARTICLE

A theoretical description of polylactic acid biodegradation in composting processes through mathematical modeling

Yvan Baldera-Moreno[1,2] | **Alejandro Rojas-Palma**[1,2] | **Rodrigo Andler**[3]

[1]Doctorado en Modelamiento Matemático Aplicado, Universidad Católica del Maule, Talca, Chile

[2]Departamento de Matemática, Física y Estadística, Universidad Católica del Maule, Talca, Chile

[3]Escuela de Ingeniería en Biotecnología, Centro de Biotecnología de los Recursos Naturales (Cenbio), Universidad Católica del Maule, Talca, Chile

Correspondence
Yvan Baldera-Moreno, Doctorado en Modelamiento Matemático Aplicado, Universidad Católica del Maule, Av San Miguel 3605, Talca, 3460000, Chile.
Email: yvan.baldera@alu.ucm.cl

Abstract

Polylactic acid (PLA) is a bio-based plastic that is biodegradable under appropriate conditions of temperature, humidity and oxygen, which are achieved in the composting process. The objective of this work is to formulate a mathematical model that predicts the biodegradation of polylactic acid in composting processes. We performed a qualitative analysis of the reduced composting mass system, which is non-linear and non-autonomous. First, the reduced model was transformed into an autonomous system, showing that their solutions are positive, bounded and non-periodic. Furthermore, it was shown that the origin is locally and globally exponentially stable, the axial equilibrium is unstable and that a degenerate transcritical bifurcation exists at the origin. Simulations of the reduced system indicated that the PLA mass is completely biodegraded when the time tends to infinity, which was shown theoretically. In addition, numerical simulations of the complete composting system were performed considering three initial values of the carbon/nitrogen ratio. It was concluded that the initial carbon/nitrogen ratio of 32.5 reached 90% of PLA biodegradation in approximately 150 days. This work provides a mathematical tool applied to the field of biotechnology of biodegradable plastics.

KEYWORDS
PLA biodegradation, C/N ratio, non-autonomous system, asymptotically autonomous system, stability

1 | INTRODUCTION

Polylactic acid (PLA) is one of the most widely used bio-based and biodegradable polymers for applications in agriculture [64], biomedicine [60] and as a packaging material [57], due to its easy availability, good biodegradability and good mechanical properties. However, the applicability of PLA has been relatively limited because its heat distortion temperature, hardness and degradation rate are unsatisfactory [21]. In addition, it is known that its degradability is null or very low if it is disposed of in natural environments [30]. According to Booth et al. (2017) [9], the rate of hydrolysis of the polymer chain also increases with temperature as it affects both the rate of oxygen diffusion and free radical formation. For this reason, in order to degrade PLA, suitable temperature conditions are required, such as those achieved in the composting process [23, 34].

Composting is currently the most used technique at the moment of valorizing organic wastes, thanks to its low operational cost and the production of a stabilized substrate, called compost [59]. Biodegradation of PLA in the composting process occurs in two steps. Initially, the heat and moisture from composting attack the PLA chains and break them apart, producing low molecular weight polymers and, eventually, lactic acid. Finally, the microorganisms present in the composting process mineralize the oligomer fragments and lactic acid to generate methane and carbon dioxide under anaerobic and aerobic conditions, respectively [41, 52]. Furthermore, the rate of PLA biodegradation depends on several influencing factors of the composting process, such as temperature, moisture content, oxygen concentration, aeration, carbon/nitrogen (C/N) ratio and pH [24].

Nowadays, there are some studies of mathematical models that evaluate the degradability of plastics based on the measurement of carbon dioxide, mass loss, Arrhenius equation, among others [4]. In the work of Baldera-Moreno et al. (2023) [5], a model of PLA biodegradation under controlled composting conditions was proposed whose degradation rates are variable with respect to

Abbreviations: PLA, polylactic acid; C/N, carbon/nitrogen ratio; ODE, ordinary differential equations.

the influencing factors; but the influence of the C/N ratio is not considered. According to Chowdhury et al. (2013) [11], the ideal range of the initial C/N ratio should be between 25 and 40 to perform well in the composting process.

The main objective of this work is to formulate a mathematical model that predicts the biodegradation of PLA in composting processes. In Section 2, the mathematical model is formulated, the assumptions of the model are presented and a schematic of the relationship between the state variables. Then, in Section 3, a qualitative analysis of the reduced composting mass model is presented and the numerical simulations that validate the previous results are also shown. Section 4, simulations of the complete composting model were performed with three different initial C/N ratios to evaluate their effect on the biodegradation of the PLA mass. Finally, the main conclusions of this work are presented in Section 5.

2 | MATHEMATICAL MODEL PROPOSAL

In this section, a mathematical model of the composting process is formulated to carry out the biodegradation of the PLA mass, by means of ordinary differential equations. In this formulation, it was considered that the degradation rates of the composting masses are variable with respect to some of the main influencing factors of the composting process (temperature, moisture content, oxygen concentration and C/N ratio).

2.1 | Multicomponent composting model

The total dry mass of composting M can be expressed as the sum of the composting mixture and the PLA mass, as shown in Equation (1) [5]:

$$\frac{dM}{dt} = \frac{dm_c}{dt} + \frac{dm_{PLA}}{dt}, \tag{1}$$

where, M is the total dry mass of composting (kg), m_c is the dry mass of the composting mixture (kg) and m_{PLA} is the dry mass of PLA (kg).

The degradation of compost dry mass has a decreasing exponential behavior, given by Equation (2) [36]:

$$\frac{dm_c}{dt} = -k_c(\cdot)\,[m_c - m_e], \tag{2}$$

where, m_c is the dry mass of the composting mixture at time t (kg), k_c is the degradation rate of the composting mixture (day^{-1}) and m_e is the equilibrium of the composting mixture (kg). This equation is often used to describe the biodegradation of different organic solid wastes such as: poultry manure [36], municipal solid waste [39], yard waste [43], food waste [37], short paper fiber [16], broiler litter [15], pig manure [29], wheat straw [49], rose pomace [19], among others.

In the Equation (1), the mass of PLA is considered as a substrate of the composting process. The biodegradation of PLA mass in the composting process is divided into two phases: slow and fast reaction phase. Initially, in the slow reaction phase the heat and moisture of the composting process attack the PLA chains and break them, producing small molecular weight polymers (oligomers or monomers) and lactic acid; and it culminates when the switching time between the phases is reached. Finally, in the fast reaction phase, the degradation rate of PLA is higher, because microorganisms begin to metabolize the small PLA fragments to generate methane and carbon dioxide under anaerobic and aerobic conditions, respectively [41, 52, 61]. Thus, the dynamics of PLA mass degradation is represented by Equation (3) [5, 50]:

$$\frac{dm_{PLA}}{dt} = -\frac{k_I(\cdot)\,m_{PLA}}{1+e^{(t-t^*)}} - \frac{k_{II}(\cdot)\,m_{PLA}\sqrt{m_{PLA,0}-m_{PLA}}}{1+e^{(t^*-t)}}, \tag{3}$$

where, m_{PLA} is the mass concentration of PLA at time t (kg), $m_{PLA,0}$ is the initial concentration of PLA (kg), t^* is the switching time between the slow and fast reaction phase (day), k_I is the slow reaction kinetic constant (day^{-1}), k_{II} is the fast reaction kinetic constant ($day^{-1} \cdot kg^{-0.5}$). In addition, the switching time, $t^* = aT + b$, depends on the temperature (T), with a and b constants. The exponential terms have been added to smooth the kinetic curves around the switching time at $t = t^*$. Indeed,it is reasonable, from a physical point of view, to consider a gradual transition between the two reaction phases when approaching the switching time [50].

In this study, we consider that the decomposition rates $k_j(\cdot)$ are variable (not constant) and take into account the effects of temperature (T), moisture content (m_{H_2O}), oxygen concentration (C_{O_2}) and Carbon/Nitogen ratio ($R_{C/N}$), we have to

$$k_j(T, m_{H_2O}, C_{O_2}, R_{C/N}) = k_{j,max} \cdot X_T \cdot X_{m_{H_2O}} \cdot X_{C_{O_2}} \cdot X_{R_{C/N}}, \qquad j = c, I, II, r, \tag{4}$$

where $k_{j,max}$ is the maximum degradation rate, and the correction factors have been taken from secondary sources [16, 13, 38, 20], given by

$$X_T = e^{-0.5\left(\left[\frac{T-57.33}{15.82}\right]^2\right)}, \tag{5}$$

$$X_{m_{H_2O}} = e^{-0.5\left(\left[\frac{m_{H_2O}-44.51}{18.73}\right]^2\right)}, \tag{6}$$

$$X_{C_{O_2}} = 0.614 \cdot \arctan(0.4 \cdot C_{O_2}), \tag{7}$$

$$X_{R_{C/N}} = e^{-0.5\left(\left[\frac{R_{C/N}-31.94)}{10.16}\right]^2\right)}. \tag{8}$$

2.2 | Energy balance

The energy balance of a composting reactor is largely determined by the extent of decomposition and its associated heat release [26]. Therefore, the heat stored in the compost (q_s) is evaluated knowing the rate of heat production in the biorector (q_g), the sensible heat of dry air (q_a) and the latent heat of water (q_w) inside and outside the system and the heat loss from the reactor wall (q_l) [39, 33, 3]. The thermal balance for a composting system is given by:

$$q_s = q_g + (q_a + q_w)_{in} - (q_a + q_w)_{out} - q_l.$$

The following equation describes the temperature (T) of the composting process, which is closely related to the thermal balance:

$$\frac{dT}{dt} = \frac{1}{Mc_p(\cdot)}\left(\Delta h_c(\cdot)\frac{dM}{dt} + \dot{m}_{in}HAI(\cdot) - \dot{m}_{out}HAO(\cdot) - UA[T - T_{amb}]\right), \tag{9}$$

where c_p is the specific heat capacity of the compost ($kJ\,kg^{-1}\,°C^{-1}$), Δh_c is heat of combustion ($kJ\,kg^{-1}$), $\dot{m}$ is the inlet and outlet airflow rate ($kg\,day^{-1}$), HAI and HAO are the inlet and outlet air enthalpies ($kJ\,kg^{-1}$), respectively, U is the overall heat transfer coefficient ($kJ\,day^{-1}\,m^{-2}\,°C^{-1}$), A is the surface area of the reactor (m^2) and T_{amb} is the ambient temperature ($°C$).

2.3 | Water balance or moisture content

The water balance of the composting based on the amount of air evaporated and the amount of water produced by microbial activity in the composting facility [39, 38], is given by:

$$\frac{dm_{H_2O}}{dt} = b_{H_2O}\frac{dM}{dt} + w_{as,in}(\cdot)\dot{m}_{in} - w_{as,out}(\cdot)\dot{m}_{out}, \tag{10}$$

where m_{H_2O} is the mass of composting water (kg), w_{as} is the absolute humidity of saturated air at local temperature ($kg\,kg^{-1}$) , b_{H_2O} is the production of water due to microbial metabolism ($kg\,kg^{-1}$).

2.4 | Oxygen concentration

The microorganisms that carry out the decomposition of the composting material are aerobic. Therefore, oxygen is necessary for aerobic biochemical reactions in the composting system. The oxygen mass balance for composting can be written considering

the oxygen accumulation in the composting matrix, the rate of oxygen mass inside and outside the matrix, and the oxygen consumption during degradation [39, 12]. The equation that describes the oxygen concentration is given by:

$$\frac{dC_{O_2}}{dt} = \frac{1}{\varepsilon V}\left(b_{O_2}\frac{dM}{dt} + \frac{\dot{m}_{in}C_{O_2,in}}{\rho} - \frac{\dot{m}_{out}C_{O_2,out}}{\rho}\right), \tag{11}$$

where C_{O_2} is the oxygen concentration in the composting matrix ($kg\ O_2\ m^{-3}\ dry\ air$), ε is the air porosity of the composting material (%), V is the volume of compost (m^3), b_{O_2} is the oxygen consumption per kg of dry mass of degradable compost ($kg\ kg^{-1}$), ρ is the density of air ($kg\ m^{-3}$).

2.5 | Carbon/nitrogen ratio

The carbon/nitrogen (C/N) ratio is the amount of carbon per unit of nitrogen that exists in a mixture. If the C/N levels are in optimal ranges (25-40:1) [15], then the temperature is maintained at levels that favor the growth of microorganisms and degradation rates are higher. In the equation that describes the C/N ratio, the effect of temperature through a first-order equation that considers the Arrhenius temperature correction method [31, 32], it is given by

$$\frac{dR_{C/N}}{dt} = -k_r(\cdot)\cdot\theta^{(T-r)}R_{C/N}, \tag{12}$$

where $R_{C/N}$ is the C/N ratio, k_r is the process rate coefficient for r days (day^{-1}), θ is the process rate.

2.6 | Scheme of the mathematical model

The mathematical model proposed describes the composting process by means of seven ODEs. The schematic representation of interaction between variables of the mathematical model can be seen in Figure 1. The boxes represent the derivative of the variables with respect to time: (i) total dry mass of composting, M; (ii) dry mass of composting mixture, m_c; (iii) dry mass of PLA, m_{PLA}; (iv) composting temperature, T; (v) moisture content of the composting, m_{H_2O}; (vi) composting oxygen concentration, C_{O_2}; (vii) composting carbon/nitrogen ratio, $R_{C/N}$.

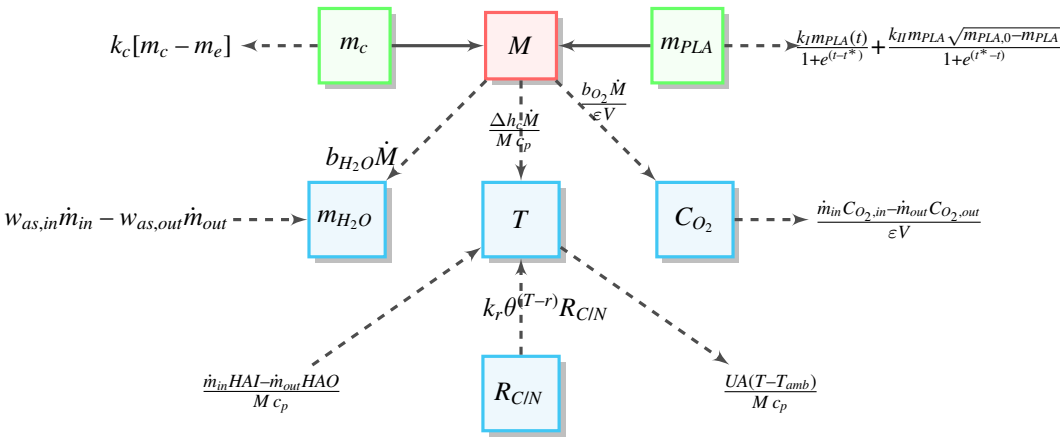

FIGURE 1 Scheme of the mathematical model (13) of the composting process. Continuous arrows indicate that the term adds to the input variable. Dashed arrows indicate positive input values and negative output values.

2.7 | Assumptions

In order to formulate the mathematical model (13) of the composting process, several assumptions were made (similar to the studies of ; Baldera-Moreno et al. (2023) [5]; Ekinci et al. (2020) [39]; Sokač et al. (2022) [54]):

1. The composting process was carried under controlled conditions.

2. Aeration during the composting process was considered constant.
3. Initial composting is a homogeneous mixture of various substrates and PLA mass.
4. The composting rate was formally expressed as the degradation rate of the dry mass, without taking the original moisture content into account.
5. Air temperature is equal to the temperature of the compost at a given location in the reactor.
6. The compost does not exceed the limits of the composting reactor.
7. Heat loss from system due to conduction and radiation is zero.
8. Compost mass is maintained at a moisture level > 40%.

2.8 | Mathematical model of the composting process

Next, taking into account the above Equations (1)-(12), the mathematical model of the composting process is presented, which is given by the system (13):

$$\begin{cases} \dfrac{dM}{dt} = \dfrac{dm_c}{dt} + \dfrac{dm_{PLA}}{dt}, \\ \dfrac{dm_c}{dt} = -k_c[m_c - m_e], \\ \dfrac{dm_{PLA}}{dt} = -\dfrac{k_I m_{PLA}}{1+e^{(t-t^*)}} - \dfrac{k_{II} m_{PLA}\sqrt{m_{PLA,0}-m_{PLA}}}{1+e^{(t^*-t)}}, \\ \dfrac{dT}{dt} = \dfrac{1}{Mc_p}\left(\Delta h_c(\cdot)\dfrac{dM}{dt} + \dot{m}_{in}HAI(\cdot) - \dot{m}_{out}HAO(\cdot) - UA(T-T_{amb})\right), \\ \dfrac{dm_{H_2O}}{dt} = b_{H_2O}\dfrac{dM}{dt} + w_{as,in}(\cdot)\dot{m}_{in} - w_{as,out}(\cdot)\dot{m}_{out}, \\ \dfrac{dC_{O_2}}{dt} = \dfrac{1}{\varepsilon V}\left(b_{O_2}\dfrac{dM}{dt} + (A\nu_{in}(\cdot) - A\nu_{out}(\cdot))C_{O_2}\right), \\ \dfrac{dR_{C/N}}{dt} = -k_r\theta^{(T-r)}R_{C/N}. \end{cases} \tag{13}$$

The system (13) is characterized by including the PLA mass as a substrate of the total composting and also considers that the degradation rates are variable taking into account the main influencing factors of the composting process. On the other hand, in system (13) a differential equation of the C/N ratio is considered to evaluate its effect on the biodegradation of PLA mass.

3 | MAIN RESULTS

Now, we will present the main results obtained in this work. First, a qualitative analysis of the reduced mathematical model of the composting masses was performed, in order to prove biodegradation of the PLA mass. Finally, simulations of the reduced system were obtained where it is validated that the PLA mass is completely biodegraded when the time tends to infinity.

3.1 | Qualitative analysis of the composting masses

In this section, a qualitative analysis of the composting mass system was performed, assuming constant degradation rates.

3.1.1 | Non-autonomous system

Due to the complexity of the complete mathematical model (13) (non linear ODE system of non-autonomous type), a qualitative analysis of the reduced composting mass system was performed. For this purpose, we assume that the value of the degradation rates are contant ($k_j = cte$) in the system (14).

$$\begin{cases} \dfrac{dm_c}{dt} &= -k_c[m_c - m_e], \\ \dfrac{dm_{PLA}}{dt} &= -\dfrac{k_I m_{PLA}}{1+e^{(t-t^*)}} - \dfrac{k_{II} m_{PLA}\sqrt{m_{PLA,0}-m_{PLA}}}{1+e^{(t^*-t)}}. \end{cases} \tag{14}$$

The above system can be written in the form of a non-homogeneous system:

$$X'(t) = A(t,X)\cdot X(t) + b \tag{15}$$

where $X = \begin{pmatrix} m_c & m_{PLA} \end{pmatrix}^T$ is the vector of composting masses,

$$A(t,X) = \begin{pmatrix} L_1 & 0 \\ 0 & L_2 \end{pmatrix} \quad \text{and} \quad b = \begin{pmatrix} k_c m_e \\ 0 \end{pmatrix}. \tag{16}$$

with $L_1 = -k_c$ and $L_2 = -\frac{k_I}{1+e^{t-t^*}} - \frac{k_{II}\sqrt{m_{PLA,0}-m_{PLA}}}{1+e^{t^*-t}}$.

The System (14) is defined in the region

$$\Omega = \left\{(m_c, m_{PLA}) \in \mathbb{R}^2 : m_c > 0, m_{PLA} \geq 0\right\} = \mathbb{R}^+ \times \mathbb{R}^+_0.$$

Now, we show that the non-homogeneous system (15) satisfies the following positivity result of solutions.

Lemma 1. *If the system* (15) *satisfies that* $X(0) \succeq \mathbf{0}$ *and* $b \succeq \mathbf{0}$*, then* $X(t) \succeq \mathbf{0}$*, for all* $t \geq 0$*.*

Proof. First, we will prove that the elements of the diagonal are non-positive. Indeed, let us note that $L_1 = -k_c \leq 0$ since $k_c > 0$. Now, let us note that the value of

$$L_2 = -\frac{k_I}{1+e^{t-t^*}} - \frac{k_{II}\sqrt{m_{PLA,0}-m_{PLA}}}{1+e^{t^*-t}} \leq 0,$$

since, if $t \to +\infty$ then

$$L_2 \to -k_{II}\sqrt{m_{PLA,0}-m_{PLA}} < 0, \forall t > 0.$$

Thus, all the elements in the diagonal of the matrix $A(t,X)$ are non-positive, i.e., $L_i \leq 0$ for $i = 1, 2$.

Also, note that all off-diagonal elements of the matrix $A(t,X)$ are zero and hence non-negative, that is, $A_{k,l} \geq 0$ for $k, l = 1, 2$, $k \neq l$. Therefore, the matrix $A(t,X)$ is a Laplacian graph.

Now, to prove positivity, let us consider any $t' \geq 0$ such that there exists $k' \in \{1, 2\}$ with $X_{k'}(t') = 0$ and such that $X(t') \succeq \mathbf{0}$, clearly, unless such t' exists. Therefore, $X(t)$ remains forever in the nonnegative cone.

Note that

$$X'_{k'}(t') = \sum_{l=1}^{2} A_{k',l}(X(t'))\cdot X_l(t') \geq 0. \tag{17}$$

because A is a graph Laplacian, so off-diagonal entries are nonnegative, see proof of the Proposition 2 in Blanes et al. 2022 [8]. Then, by Equations (17) and (16), we have that

$$X'_{k'}(t') = \sum_{l=1}^{2} A_{k',l}(X(t'))\cdot X_l(t') + b_{k'} \geq 0.$$

Thus, $X_{k'}$ cannot change sign at t', i.e. any state variable $X_{k'}(t) \geq 0$ for all $t \geq 0$. Therefore, $X(t) \succeq \mathbf{0}$ for all $t \geq 0$. □

3.1.2 | Autonomous system

Note that, the system of mass of composting (14) is decoupled. Therefore, the composting mass systems will be qualitatively studied separately. It is well known that, the solution of the equation (2) has an exponentially decreasing behavior, and is given by the Equation (18):

$$m_c(t) = [m_c(0) - m_e]e^{-k_c t} + m_e, \quad \forall t \geq 0. \tag{18}$$

Also, if $t = 0$ then $m_c = m_c(0)$ and if $t \to \infty$ then $m_c = m_e > 0$, i.e., the solution $m_c(t)$ is positive and bounded for all $t \geq 0$.

Note that, the Equation (3) is a non-autonomous and non-linear ODE. Classical theory suggests that any non-autonomous system can be viewed as autonomous by considering time as another dependent variable (to eliminate its explicit dependence)

and adding an additional differential equation to the dynamical system. This standard transformation converts a non-autonomous system to autonomous. But this argument is not very useful, since the usual techniques for the study of autonomous systems, such as local stability of equilibrium points, local bifurcations and other methods, cannot be applied.

For our purpose, an alternative transformation was considered to convert the Equation (3) into a system of autonomous ODEs with equilibrium points, similar to that proposed in the work of Ben-Tal (2021) [6]. Now, considering the change of variable $v(t) = e^{t^*-t}$ we obtain the following autonomous system given by

$$\begin{cases} \dfrac{dm_{PLA}}{dt} &= -\dfrac{k_I\, v\, m_{PLA}}{1+v} - \dfrac{k_{II} m_{PLA}\sqrt{m_{PLA,0}-m_{PLA}}}{1+v}, \\ \dfrac{dv}{dt} &= -v. \end{cases} \tag{19}$$

The System (19) is defined in the region

$$\overline{\Omega} = \left\{(m_{PLA}, v) \in \mathbb{R}^2 : m_{PLA} \geq 0, v > 0\right\}. = \mathbb{R}_0^+ \times \mathbb{R}^+.$$

The system parameters (19) are all positive, that is,

$$k = (k_I, k_{II}, m_{PLA,0}) \in (\mathbb{R}^+)^3.$$

The equilibria of the autonomous system (19) are given by

$$M_0 = (0, 0)$$

and

$$M_1 = (m_{PLA,0}, 0).$$

Remark 1. The values of the degradation rates k_j (4) depend on several influencing factors. Thus, some may be zero at some moment in time. In practice this does not occur since it would imply that there is no degradation. However, in this paper we include the case when $k_{II} = 0$ to study the influence of bifurcation on the dynamics of the autonomous system (19).

Remark 2. The autonomous System (19) is of Kolmogorov type. Therefore, the coordinate axes are invariant sets.

Next, we show that the solutions of the autonomous System (19) are bounded.

Lemma 2. *The solutions of the autonomous System* (19) *are uniformly bounded.*

Proof. First, let us note that from the second equation of the System (19), we have that $0 \leq v \leq L$, where $L = v(0)$. Now, we have to

$$\begin{aligned} 1 \leq & 1 + v \leq 1 + L \\ \frac{1}{1+L} \leq & \frac{1}{1+v} \leq 1 \end{aligned}$$

Thus, we have that

$$\frac{v}{1+v} \leq L.$$

On the other hand,

$$\sqrt{m_{PLA,0} - m_{PLA}} \leq \sqrt{m_{PLA,0}} =: M.$$

Now, let $Z = m_{PLA} + v$, then

$$\begin{aligned}
\frac{dZ}{dt} =& \frac{dm_{PLA}}{dt} + \frac{dv}{dt} \\
\frac{dZ}{dt} =& -\left(\frac{k_I\, v}{1+v} + \frac{k_{II}\sqrt{m_{PLA,0} - m_{PLA}}}{1+v} \right) m_{PLA} - v \\
\frac{dZ}{dt} \leq& -\delta\, m_{PLA} - v \\
\frac{dZ}{dt} \leq& -\delta Z
\end{aligned}$$

which is a first order differential inequality with

$$\delta := k_I L + k_{II} M > 0. \tag{20}$$

Applying the comparison theorem for differential inequalities (Page 30 in [7]), we get that $0 \leq Z(t) \leq e^{-\delta t}$. Thus, we have that

$$0 \leq Z(t) \leq \max\left\{1, e^{-\delta t}\right\}.$$

Therefore, the solutions of the autonomous system (19) are uniformly bounded. □

The following result makes use of the Bendixson-Dulac criterion and the form of the Kolmogorov type system to show that the system (19) has no periodic orbits.

Lemma 3. *There are no periodic solutions of the autonomous system* (19).

Proof. Note that, the system (19) can be expressed in the form $X' = F(X)$ where $X = (m_{PLA}, v)^T$ and $F(X) = (f_1, f_2)^T$, with

$$f_1(X) = -\frac{k_I\, v\, m_{PLA}}{1+v} - \frac{k_{II} m_{PLA}\sqrt{m_{PLA,0} - m_{PLA}}}{1+v}$$

and

$$f_2(X) = -v.$$

We will use the Bendixson-Dulac criterion [48] considering the function

$$h(X) = \frac{1}{m_{PLA}\, v} > 0,$$

for all X at inside the region $\overline{\Omega}$.

Now, let $\nabla \cdot (hF)$ the divergence of vector field hF, defined by

$$\nabla \cdot (hF)(X) = \frac{d}{dm_{PLA}}(f_1(X)h(X)) + \frac{d}{dv}(f_2(X)h(X)).$$

Thus, we have

$$\begin{aligned}
\nabla \cdot (hF)(X) =& \frac{d}{dm_{PLA}}\left(-\frac{k_I}{1+v} - \frac{k_{II}\sqrt{m_{PLA,0} - m_{PLA}}}{v(1+v)} \right) + \frac{d}{dv}\left(-\frac{1}{m_{PLA}} \right) \\
=& \frac{k_{II}}{2\sqrt{m_{PLA,0} - m_{PLA}}(v + v^2)}.
\end{aligned}$$

Then, $\nabla \cdot (hF) > 0$ for all (m_{PLA}, v) at inside the first quadrant. Therefore, by the Bendixson-Dulac criterion [48, 10], has no periodic solutions (or limit cycles) within the first quadrant. □

Remark 3. The system (19) has equilibrium in the origin $M_0 = (0, 0)$, but the system is not defined at this point, since $v(t) = e^{t^* - t}$ cannot be zero. However, using what was proposed in the work of Markus [42] and Thieme [58], we will show that when t tends to infinity the system is an asymptotically autonomous system and that the origin is locally asymptotically stable.

Definition 1 (Markus, 1956 [42])**.** An ordinary differential equation in $\mathbb{R}^n$,

$$\dot{x} = f(t, x), \tag{21}$$

is called asymptotically autonomous –with limit equation (22)–

$$\dot{y} = g(y), \tag{22}$$

if

$$f(t,x) \to g(x), \qquad t \to \infty, \qquad \text{locally uniformly in } x \in \mathbb{R}^n,$$

i.e., for x in any compact subset of $\mathbb{R}^n$.

Let's note that, the solution of the second equation of the system (19) is given by

$$v(t) = v(0)e^{-t+c}, \qquad c = t^*$$

or

$$v(t) = e^{-t+t^*}.$$

Now, if we substitute the above solution into the first equation of the system (19) and making that $t \to \infty$, then we have that the system (19) is equivalent to an asymptotically autonomous system, which has the limiting system (23), given by

$$\frac{dm_{PLA}}{dt} = -k_{II} m_{PLA} \sqrt{m_{PLA,0} - m_{PLA}}. \tag{23}$$

Clearly, the equilibria of the limit system are

$$m^*_{PLA} = 0$$

and

$$m^{**}_{PLA} = m_{PLA,0}.$$

Now, we present a result about the stability of origin of system (19).

Proposition 1. *The origin $M_0 = (0,0)$ of the system* (19) *is an equilibrium point locally asymptotically stable.*

Proof. First, we determine the Jacobian DF of the system (23), which is given by

$$DF(m_{PLA}) = k_{II} \frac{3m_{PLA} - 2m_{PLA,0}}{2\sqrt{m_{PLA,0} - m_{PLA}}} \tag{24}$$

Now, we evaluate the equilibrium point $m^*_{PLA} = 0$ in (24), we obtain that

$$DF(0) = -k_{II} \sqrt{m_{PLA,0}} < 0,$$

that is, the eigenvalue is negative. Therefore, the equilibrium $m^*_{PLA} = 0$ of limit system (23) is locally asymptotically stable. Moreover, by Lemma 1 and Lemma 2 we have that the solutions of system (19) are bounded and that there are no periodic orbits for all $t \geq 0$, respectively. Therefore, applying Theorem 1.2, 1.3 and 1.5 [58], we have that the origin $M_0 = (0,0)$ of the system (19) is an equilibrium point locally asymptotically stable. □

Now, we show the global exponential stability of the origin of the autonomous system (19), by means of a Lyapunov function.

Theorem 1. *The origin $M_0 = (0,0)$ of the autonomous system* (19) *is globally exponentially stable.*

Proof. Since (19) is a Kolmogorov type system, we will consider the Lyapunov function given by

$$V(X) = m^2_{PLA} + v^2.$$

Clearly $V(X) > 0$, for all $m_{PLA} \neq 0$ and $v \neq 0$.

Deriving the function V with respect to t, we have:

$$\begin{aligned}\frac{\partial V}{\partial t} =& \frac{\partial V}{\partial m_{PLA}}\frac{\partial m_{PLA}}{\partial t} + \frac{\partial V}{\partial v}\frac{\partial v}{\partial t}\\ =&(2m_{PLA})\left(-\frac{k_I\, v\, m_{PLA}}{1+v} - \frac{k_{II} m_{PLA}\sqrt{m_{PLA,0}-m_{PLA}}}{1+v}\right) + (2v)(-v)\\ =&-2m_{PLA}^2\left(\frac{k_I\, v}{1+v} + \frac{k_{II}\sqrt{m_{PLA,0}-m_{PLA}}}{1+v}\right) - 2v^2\end{aligned}$$

Then $\frac{\partial V(X)}{\partial t} < 0$ for all $m_{PLA} \neq 0$ and $v \neq 0$. Thus $V(X)$ is a suitable Lyapunov function [28], since it is positive definite, decreasing and strictly decreasing.

Now, note that

$$k_1\|X\|^a \leq V(X) \leq k_2\|X\|^a,$$

where $k_1 = \frac{1}{2}$, $k_2 = 2$ and $a = 2$. In addition

$$\begin{aligned}\frac{\partial V}{\partial t} + \frac{\partial V}{\partial X}f(t,X) =& -4m_{PLA}^2\left(\frac{k_I\, v}{1+v} + \frac{k_{II}\sqrt{m_{PLA,0}-m_{PLA}}}{1+v}\right) - 4v^2\\ \leq& -4K(m_{PLA}^2 + v^2) \leq -k_3\|X\|^a,\end{aligned}$$

where $K = \max\{\delta, 1\}$, with δ defined in (20) and $k_3 = 4K$. Therefore, the origin $M_0 = (0,0)$ equilibrium point is globally exponentially stable, by Theorem 4.10 [40]. □

Remark 4. The above result implies that the mass of PLA degrades asymptotically and also exponentially, i.e., it tends to zero rapidly.

Remark 5. Observe that, if we evaluate the equilibrium point $m_{PLA}^{**} = m_{PLA,0}$ in (24) then DF is indeterminate. However, using the blow up technique we will show that the axial equilibrium point $M_1 = (m_{PLA,0}, 0)$ is unstable.

Theorem 2. *If $m_{PLA,0} < \frac{1}{k_{II}^2}$, then the axial equilibrium point $M_1 = (m_{PLA,0}, 0)$ of the autonomous system* (19) *is unstable.*

Proof. First, we calculate the Jacobian matrix of the system (19), given by

$$DF(m_{PLA}, v) = \begin{pmatrix} DJ(m_{PLA}, v)_{11} & \frac{k_{II} m_{PLA}\sqrt{m_{PLA,0}-m_{PLA}} - k_I m_{PLA}}{(v+1)^2} \\ 0 & -1 \end{pmatrix}. \tag{25}$$

Clearly, the Jacobian matrix evaluated at the point $(m_{PLA,0}, 0)$ is not defined, since

$$DF(m_{PLA}, v)_{11} = \frac{1}{2v+2}\left(-2k_I v + \frac{3k_{II} m_{PLA} - 2k_{II} m_{PLA,0}}{\sqrt{m_{PLA,0}-m_{PLA}}}\right). \tag{26}$$

To overcome this difficulty, we will use the method of blowing-up in the v-direction with the change of variables $m_{PLA} = (m_{PLA,0} - x)y$ and $v = y$. Thus, the new system is given by

$$\begin{cases} \dfrac{dx}{dt} &= \frac{(m_{PLA,0}-x)\left(k_{II}\sqrt{m_{PLA,0}(1-y)+xy}+(k_I-1)y-1\right)}{y+1}, \\ \dfrac{dy}{dt} &= -y. \end{cases} \tag{27}$$

Hence, evaluating the point $(m_{PLA,0}, 0)$ the Jacobian matrix of the above system (27), we obtain that

$$DX(m_{PLA,0}, 0) = \begin{pmatrix} 1 - k_{II}\sqrt{m_{PLA,0}} & 0 \\ 0 & -1 \end{pmatrix}. \tag{28}$$

Therefore, if $m_{PLA,0} < \frac{1}{k_{II}^2}$, then the axial equilibrium point $M_1 = (m_{PLA,0}, 0)$ of the autonomous system (19) is unstable. □

3.1.3 | Bifurcation of codimension one with an eigenvalue equal to zero

Next, we will show under what conditions a transcritical bifurcation occurs at the equilibrium point $M_0 = (0,0)$ of the three-parameter autonomous system (19).

The system (19) can also be written as a k-parameterized system:

$$x' = F(x,k), \tag{29}$$

where $x = (m_{PLA}, v) \in \mathbb{R}_0^+ \times \mathbb{R}^+$ and $k = (k_I, k_{II}, m_{PLA,0}) \in \mathbb{R}^+ \times \mathbb{R}_0^+ \times \mathbb{R}^+$.

Theorem 3. *The parameterized autonomous system* (29)*, has a transcritical bifurcation at the equilibrium point* $M_0 = (0,0)$ *when the parameter k passes through the bifurcation value* $k_0 = \left(k_I, 0, m_{PLA,0}\right)$*:*

Proof. Note that, the eigenvalues of the Jacobian matrix, DF (25), evaluated at the equilibrium point $M_0 = (0,0)$, are given by $\lambda_1 = -1$ and $\lambda_2 = -k_{II}\sqrt{m_{PLA,0}}$. If we consider that $k_{II} = 0$, then $\lambda_2 = 0$, that is, there is a null eigenvalue. This shows that $(M_0, k_0) = \left(0, 0, k_I, 0, m_{PLA,0}\right)$ is a non-hyperbolic equilibrium point of codimension one, since $F(M_0, k_0) = (0 \;\; 0)^T$ and

$$DF(M_0, k_0) = \begin{pmatrix} 0 & 0 \\ 0 & -1 \end{pmatrix}.$$

Where $v_0 = (1 \quad 0)^T$ and $w_0 = (1 \quad 0)^T$ are the right and left eigenvectors corresponding to $\lambda_2 = 0$, respectively. In addition, it follows that

$$D_2F(M_0, k_0) = \begin{pmatrix} \begin{pmatrix} 0 & -k_I \\ -k_I & 0 \end{pmatrix} \begin{pmatrix} 0 & 0 \\ 0 & 0 \end{pmatrix} \end{pmatrix}$$

$$F_k(M_0, k_0) = \begin{pmatrix} 0 & 0 & 0 \\ 0 & 0 & 0 \end{pmatrix}$$

$$F_{kx}(M_0, k_0) = \begin{pmatrix} 0 & -\sqrt{m_{PLA,0}} & 0 \\ 0 & 0 & 0 \end{pmatrix}$$

Thus, we have that

$$a = w_0^T F_k(x_0, k_0) = \begin{pmatrix} 0 \\ 0 \\ 0 \end{pmatrix},$$

$$b = (w_0^T D^2 F(x_0, k_0))(v_0, v_0) = \begin{pmatrix} 0 \\ -k_I \end{pmatrix} \neq \begin{pmatrix} 0 \\ 0 \end{pmatrix},$$

$$c = -(w_0^T D^2 F(x_0, k_0))(v_0, P_0) J_s^{-1} Q_0 F_k(x_0, k_0) + v_0^T (w_0^T F_{kx}(x_0, k_0))^T$$

$$= \begin{pmatrix} 0 \\ -\sqrt{m_{PLA,0}} \\ 0 \end{pmatrix} \neq \begin{pmatrix} 0 \\ 0 \\ 0 \end{pmatrix}.$$

Therefore, applying Sotomayor's Theorem 4, we have that there is a transcritical bifurcation at the equilibrium point $M_0 = (0,0)$ when the parameter k passes through the bifurcation value $k_0 = \left(k_I, 0, m_{PLA,0}\right)$. □

3.2 | Numerical simulation of the autonomous system

In this section, numerical simulations have been carried out in order to validate the results obtained in our qualitative analysis of the autonomous system (19).

In Figure 2, we can see that the equilibrium point $M_0 = (0,0)$ of the System (19) is locally and globally asymptotically stable, as was demonstrated in Theorems 1 and 1, respectively. This means that, the mass of PLA is completely biodegraded in the composting process, when $t \to \infty$. Furthermore, we can see that the solutions are positive, bounded and that there are no periodic orbits, as proved in Lemmas 1, 2 and 3, respectively. Whereas, solutions close to the axial equilibrium point $M_1 = (m_{PLA,0}, 0)$ move away from it, since it is an unstable equilibrium, as proved in Theorem 2.

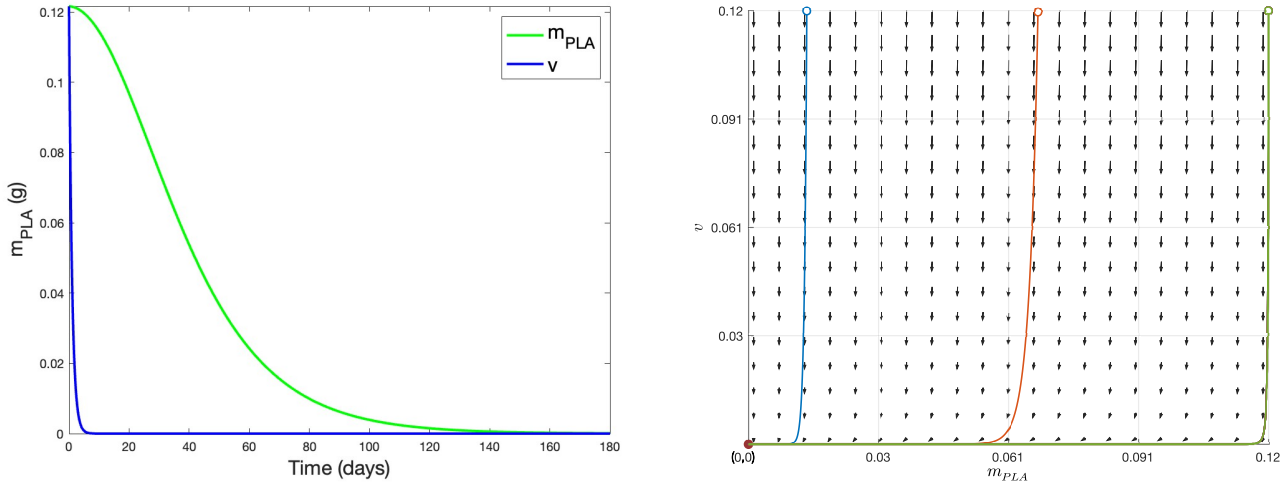

(a) (b)

FIGURE 2 For $k_I = 0.0024$, $k_{II} = 0.1375$, $m_{PLA,0} = v(0) = 0.1216$: (a) Solutions of $m_{PLA}(t)$ and $v(t)$ tend to the equilibrium point $M_0 = (0, 0)$ of the system (19), which is locally and globally asymptotically stable. (b) Phase portrait of the System (19) for different initial conditions: (0.012,0.1216), (0.069,0.1216), (0.1216,0.1216); which validates that the origin is globally exponentially stable. This means that, if $t \to \infty$ then the mass of PLA is fully biodegraded in the composting process.

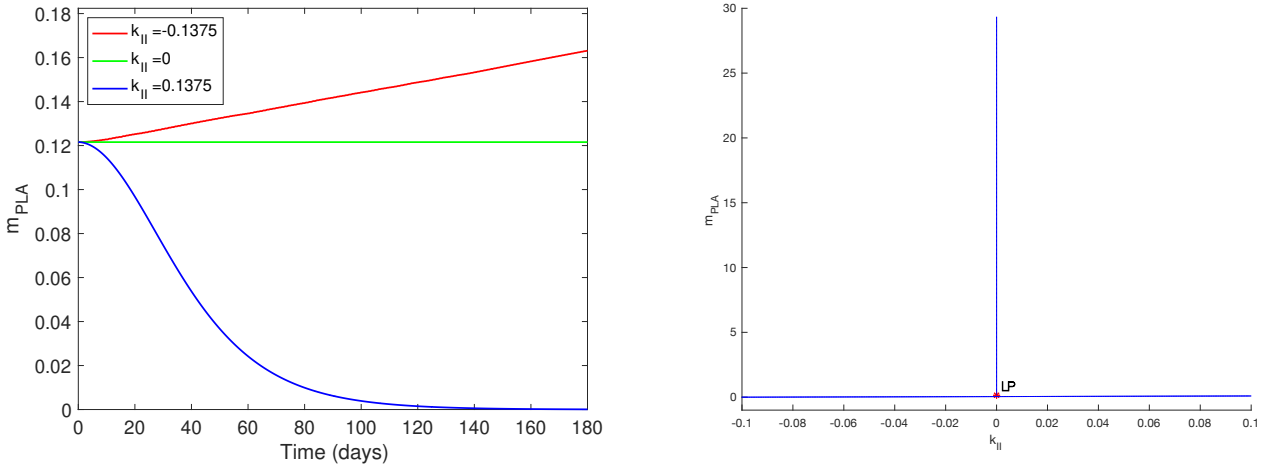

(a) (b)

FIGURE 3 (a) Solutions of $m_{PLA}(t)$ with $k_I = 0.0024$, $m_{PLA,0} = v(0) = 0.1216$ and $k_{II} = –0.1375,\ 0,\ 0.1375$. (b) Degenerate transcritical bifurcation diagram of the autonomous system (19).

Figure 3(a), shows the dynamics of the PLA mass for a negative, zero and positive value of k_{II}, which suggests that it is a bifurcation parameter. In Figure 3(b), the degenerate transcritical bifurcation diagram of the equilibrium $M_0 = (0, 0)$ when the parameter $k_{II} = 0$ is shown, as proved in Theorem 3. In addition, Figure 4 clearly shows the change in the stability of the equilibria $M_0 = (0, 0)$ and $M_1 = (m_{PLA,0}, 0)$. Note that, if $k_{II} = –0.1375 < 0$ then $M_0 = (0, 0)$ is unstable. Whereas if $k_{II} = 0$ then the m_{PLA}-axis is a straight of stable equilibria, i.e.,there are infinite equilibrium points. Finally, if $k_{II} = 0.1375 > 0$ then all solutions of system (19) tend to the origin asymptotically.

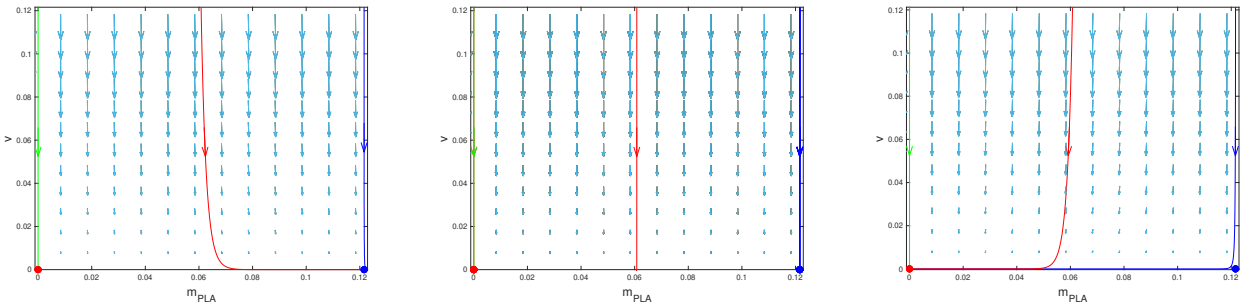

(a) (b) (c)

FIGURE 4 Portrait phase of autonomous system (19). (a) k_{II} = –0.1375. (b) k_{II} = 0. (c) k_{II} = 0.1375.

4 | EFFECTS OF INITIAL C/N RATIO ON PLA MASS BIODEGRADATION

In this section, the simulations of the complete mathematical model (13) of the composting process are shown (see Figure 5). In order to decrease the biodegradation time of the PLA mass, three levels of initial C/N ratio (25, 32.5, 40) were considered. In Table 1, the notations for each variable and their initial values are described. In addition, the values of the parameters used to perform the numerical simulations are detailed in Table 2, which are mostly taken from secondary sources [5, 36, 39, 16, 15, 50, 13, 38, 17, 35, 46, 56, 14].

TABLE 1 Notation, description, and initial value of each variable.

Notation	Description	Initial value
M	Total dry mass of composting	$1\,kg$
m_c	Dry mass of composting mixture	$0.8\,kg$
m_{PLA}	Dry mass of PLA	$0.2\,kg$
T	Composting temperature	$25.37°C$
m_{H_2O}	Moisture content of the composting	45 %
C_{O_2}	Composting oxygen concentration	$21\,kg\,O_2\,m^{-3}$
$R_{C/N}$	Composting C/N ratio	25, 32.5, 40[a]

[a]We used three initial C/N ratios to carry out the simulations.

TABLE 2 Notation, value, unit and description for each parameter.

Notation	Value	Unit	Description
b_{H_2O}	0.51	$kg\,H_2O\,kg\,air^{-1}$	Water production coefficient
b_{O_2}	1.177	$kg\,O_2\,kg\,compost^{-1}$	Utilization rate of O_2 of compost mixture
h_c	15000.986	$kJ\,kg\,compost^{-1}$	Combustion heat of the compost mixture
$k_{c,max}$	0.0135	day^{-1}	Maximum degradation rate of composting mixture
$k_{I,max}$	0.0025	day^{-1}	Maximum degradation rate of the slow reaction phase of PLA
$k_{II,max}$	0.14758	$day^{-1}kg^{-0.5}$	Maximum degradation rate of the fast reaction phase of PLA
$k_{r,max}$	0.39	day^{-1}	Maximum process rate coefficient
θ	0.799	–	Process rate C/N ratio
t^*	40	day	Switching time from slow to fast reaction
T_{amb}	25.57	$°C$	Ambient temperature
UA	3.1046	$kJ\,day^{-1}\,°C^{-1}$	Overall heat transfer coefficient per reactor area

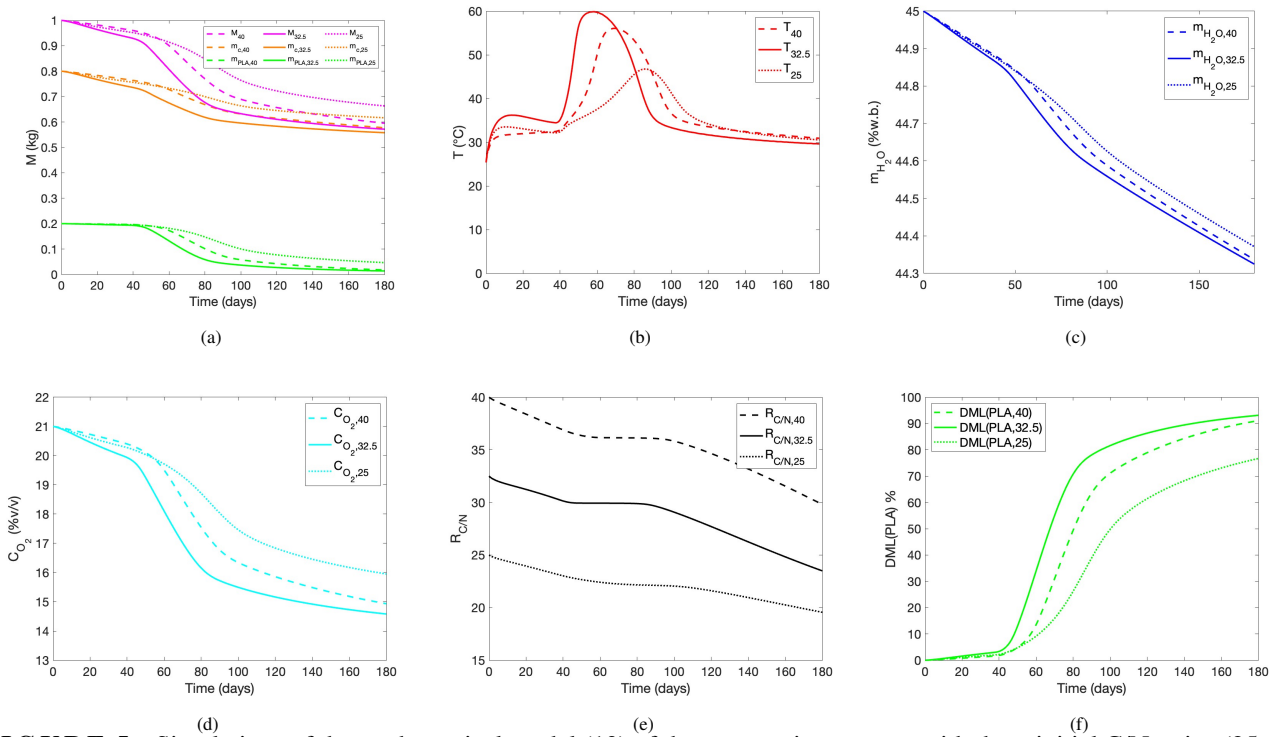

FIGURE 5 Simulations of the mathematical model (13) of the composting process with three initial C/N ratios (25, 32.5, 40). (a) Composting mass degradation. (b) Temperature. (c) Moisture content. (d) Oxygen concentration. (e) C/N ratio. (f) Dry mass loss of PLA.

4.1 | Degradation of composting masses

In Figure 5(a), the degradation behavior of the total composting dry mass (M), which is composed of the mixture of the compost dry mass (m_c) and the PLA dry mass (m_{PLA}) is described; considering three different values of initial C/N ratio: 25, 32.5, 40. Note that, if the composting process starts with an initial C/N ratio of 32.5 then all the composting masses degrade faster. Next, if the initial C/N ratio is increased to 40, then the degradation rates of the masses decrease. Finally, the lowest composting mass degradation is obtained if we consider an initial C/N ratio of 25. Furthermore, note that the degradation of the PLA mass (m_{PLA}) changes the behavior of the other masses. This is due to the fact that PLA biodegradation is divided into three phases: At the beginning of the composting process, PLA biodegradation is slow (0-40 days), since in this lag stage the microbial population must adapt to the polymer and fragment it into smaller sections (oligomers or monomers) [61]. Then, the biodegradation phase begins (40-150 days) where the adapted microbial population starts to metabolize the small particles at a higher rate. Finally, the process culminates in the plateau phase (150-180 days) where composting stabilizes [41, 22].

4.2 | Composting temperature

In Figure 5(b), the composting temperature (T) curves with different initial C/N ratios of 25, 32.5, 40 are observed. Clearly, the curve that reaches the highest temperatures is the one that starts with a C/N ratio of 32.5, followed by the initial C/N ratio of 40 and 25, respectively. Note that, the composting process starts with mesophilic temperatures and after exceeding the switching time of 40 days, all three curves begin to rise in temperature and achieve thermophilic levels which lasted approximately 2 months, favoring microbial growth and PLA biodegradation. This may explain why the composting process originated with a C/N ratio of 32.5 showed the highest loss of organic matter [62]. Finally, the composting process culminates with the final mesophilic phase, where the compost mass cools down and stabilizes at room temperature. The composting process with lower initial C/N (25) showed the lowest maximum temperature due to lower microbial activity caused by a limited supply of readily available carbon sources in the composting with lower initial C/N [63]. Therefore, we can conclude that the optimal initial C/N

ratio is 32.5, because at that level the PLA mass biodegrades faster due to the high temperatures reached by the composting process. Moreover, we should mention that the model indicates that if the initial C/N ratio is higher than 40 or lower than 25, then the maximum temperatures of the composting process will decrease. This result is similar to that obtained in composting experiments with various initial C/N ratios in diverse investigations [65, 47].

4.3 | Moisture content of the composting

The time variation of the moisture content curves (m_{H_2O}) of the composting process is shown in Figure 5(c). We can observe that the moisture content with decreases more with an initial C/N ratio of 32.5, since in this case the maximum temperature is the highest with respect to the other levels. Also, it can be noted that the initial C/N ratio slightly affects the moisture content of the composting process.

4.4 | Composting oxygen concentration

For the correct development of the composting process it is necessary to ensure the presence of oxygen, since the microorganisms that are charged with degrading the composting mass are aerobic. In Figure 5(d), it is observed that the oxygen concentration (C_{O_2}) starts to decrease slightly in all three cases, until the switching time of 40 days is reached. Then, it decreases at a faster rate because it reaches the thermophilic phase of the composting process and the microorganisms consume more oxygen. Finally, when the composting mass stabilizes at room temperature then the oxygen concentration also stabilizes. Note that, with an initial C/N ratio of 32.5 the oxygen concentration decreased the most, because in this case the maximum temperature was the highest. While with an initial C/N ratio of 25, the final oxygen concentration was the lowest, since in this case the maximum temperature was the lowest and the microorganisms do not consume much oxygen.

4.5 | Composting carbon/nitrogen ratio

Among the different factors influencing the composting process, the initial C/N ratio is one of the most important, since it provides the nutrients needed by the microorganisms to develop. Figure 5(e), shows the variation of the C/N ratio with respect to time. The behavior of the C/N ratio is decreasing and this is mainly affected by the temperature of the composting process. The C/N ratio of the three curves decreases slowly until the switching time of 40 days is reached. In the thermophilic phase, the C/N ratios in all three cases decrease very slowly. Finally, in the cooling phase, the C/N ratio has a higher degradation rate and at the end of the 180-day composting process, the C/N ratio in the three cases has decreased by approximately 30%. Thus, if the initial values of the C/N ratio are higher than 40 or lower than 25, then inconveniences related to a slower biodegradation or the decrease of the maximum temperature of the composting process may occur, this is due to the fact that the microorganisms do not find the necessary nutritional conditions as we have discussed previously. Whereas, according to our model, the best initial C/N ratio is 32.5. The C/N ratio simulations produced in our model are similar to laboratory experiments of the composting process obtained in several investigations [27, 45, 18].

4.6 | Dry mass loss of PLA

The PLA's dry mass loss (DML) was estimated from Equation (30) [51]:

$$DML(\%) = \frac{m_{PLA,0} - m_{PLA,f}}{m_{PLA,0}} \times 100 \tag{30}$$

where $m_{PLA,0}$ and $m_{PLA,f}$ are the initial and final dry mass of the PLA.

In Figure 5(f), the PLA biodegradation percentage is observed, which is calculated by Equation (30) above. It is clear that, in the lag phase the biodegradation is very slow in the three curves, since the mesophilic temperatures are low, and at this stage the plastic has not yet fragmented into small pieces. After reaching the switching time of 40 days, it can be seen that the PLA biodegradation phase begins, which is carried out at higher rates, this is due to the fact that the thermophilic temperatures are higher in this phase. Note that, according to the simulations of the model (13), the best initial C/N ratio is 32.5 since it

reaches 90% biodegradation of PLA in approximately 150 days. However, if the initial C/N ratio is increased to 40 then the 90% biodegradation of PLA is reached in almost 180 days of the composting process. Whereas, if we decrease the initial C/N ratio to 25 then the percentage of biodegradation decreases and 90% is not reached. These results show that the initial C/N ratios of 32.5 and 40 are suitable to prove that PLA is a biodegradable plastic as stipulated by the standards ISO 14855 [22], EN 14806 [1] and ISO 20200 [53]. Therefore, it is possible to confirm that the C/N ratio of the initial compost conditioned the biodegradation time of PLA, reaching 90% before 180 days in those materials with an initial C/N ratio of 32.5 and 40; while the initial composting with a C/N ratio of 20 does not reach 90% of biodegradation at the end of the process in 180 days.

5 | CONCLUSIONS

In this work, a mathematical model of PLA biodegradation in composting processes was formulated. The model consists of seven ordinary differential equations, which was characterized by including the PLA mass as a substrate of the total composting and also considers that the degradation rates of the masses are variable taking into account the main influencing factors of the composting process (temperature, moisture content, oxygen concentration, C/N ratio).

A qualitative analysis was performed on the reduced composting mass model, which is non-linear and non-autonomous. This system was transformed to autonomous, through a transformation similar to the one proposed in [6], obtaining a bidemensional system with two equilibrium points: origin $M_0 = (0, 0)$ and an axial equilibrium $M_1 = (m_{PLA,0}, 0)$. Then, it was shown that the autonomous system has non-negative, bounded solutions and that there are no periodic orbits by means of the Dulac criterion. It was proved that the origin is a locally and globally exponentially stable equilibrium point; and that the axial equilibrium is unstable, by linearization and a Lyapunov approach. It was shown that if the parameter $k_{II} = 0$ then a degenerate transcritical bifurcation exists at the origin using Sotomayor's Theorem generalized to m-parameterized functions 4 (Appendix B). Also, numerical simulations were carried out using Matlab software to validate the results obtained above and it was concluded that the mass of PLA tends to zero rapidly when $t \to \infty$, i.e., the mass of PLA can be fully biodegraded in the composting process when time tends to infinity as desired.

On the other hand, numerical simulations of the complete mathematical model of the composting process were performed. Three initial C/N ratios of 25, 32.5 and 40 were used to evaluate their effects for the biodegradation of the PLA mass over time. The results of the model simulations indicated that the initial C/N ratio of 32.5 showed higher and faster biodegradation rates in comparison with the other C/N ratios. The maximum temperature was achieved at this conditions and a 90% of biodegradation of the PLA mass was reached in approximately 150 days. Whereas, if the initial values of the C/N ratio are higher than 40 or lower than 25, disadvantages may occur, such as slower degradation of the process and a decrease of the maximum composting temperature. The above implies a decrease in the percentage of PLA biodegradation, which may be due to the fact that microorganisms do not find the necessary nutritional conditions to develop.

This work provides a mathematical tool applied to the field of biotechnology of biodegradable plastics and shows that the biodegradation time of PLA can be decreased if the composting process is initiated with an adequate C/N ratio.

AUTHOR CONTRIBUTIONS

Yvan Baldera-Moreno: Conceptualization, Methodology, Software, Validation, Formal analysis, Writing - Original Draft. Alejandro Rojas-Palma: Conceptualization, Methodology, Validation, Formal analysis, Visualization, Supervision, Writing - Review & Editing. Rodrigo Andler: Conceptualization, Methodology, Validation, Formal analysis, Visualization, Supervision, Writing - Review & Editing.

ACKNOWLEDGMENTS

Yvan Baldera-Moreno thank the "Doctoral Scholarship", awarded by the Vicerectoría de Investigación y Postgrado, Universidad Católica del Maule, Talca, Chile. Rodrigo Andler thank research project Fondecyt, grant number 1230313, from ANID, Chile. Alejandro Rojas-Palma was partially funded by UCM-IN-23202 internal grant.

CONFLICT OF INTEREST

The authors declare no potential conflict of interests.

REFERENCES

1. D. Adamcová, J. Zloch, M. Brtnický, and M. D. Vaverková, *Biodegradation/disintegration of selected range of polymers: impact on the compost quality*, Journal of Polymers and the Environment **27** (2019), 892–899.

2. D. Baca Carrasco, *Análisis y control de bifurcaciones estacionarias*, Master's thesis, Universidad de Sonora, 2009.
3. P. D. Bach, K. Nakasaki, M. Shoda, and H. Kubota, *Thermal balance in composting operations*, Journal of Fermentation Technology **65** (1987), no. 2, 199–209.
4. Y. Baldera-Moreno, V. Pino, A. Farres, A. Banerjee, F. Gordillo, and R. Andler, *Biotechnological aspects and mathematical modeling of the biodegradation of plastics under controlled conditions*, Polymers **14** (2022), no. 3, 375.
5. Y. Baldera-Moreno, A. Rojas-Palma, R. Andler, and L. Cuesta-Herrera, *Mathematical model of polylactic acid biodegradation under controlled composting conditions*, Journal of Physics: Conference Series **2515** (2023), no. 1, 012004. URL https://dx.doi.org/10.1088/1742-6596/2515/1/012004.
6. A. Ben-Tal, *Useful transformations from non-autonomous to autonomous systems*, *Physics of Biological Oscillators: New Insights into Non-Equilibrium and Non-Autonomous Systems*, Springer, 2021. 163–174.
7. G. Birkhoff and G. Rota, *Ordinary Differential Equations*, Wiley, 1991. URL https://books.google.cl/books?id=YBjEQgAACAAJ.
8. S. Blanes, A. Iserles, and S. Macnamara, *Positivity-preserving methods for ordinary differential equations*, ESAIM: Mathematical Modelling and Numerical Analysis **56** (2022), no. 6, 1843–1870.
9. A. Booth et al., *Microplastic in global and norwegian marine environments: Distributions, degradation mechanisms and transport*, Miljødirektoratet M-918 (2017), 1–147.
10. C. Chicone, *Ordinary differential equations with applications (2006)*, Texts in applied mathematics, Springer (2006).
11. A. K. M. M. B. Chowdhury, C. S. Akratos, D. V. Vayenas, and S. Pavlou, *Olive mill waste composting: A review*, International Biodeterioration & Biodegradation **85** (2013), 108–119.
12. K. Das and H. Keener, *Numerical model for the dynamic simulation of a large scale composting system*, Transactions of the ASAE **40** (1997), no. 4, 1179–1189.
13. K. Ekinci, *Theoretical and experimental studies on the effects of aeration strategies on the composting process*, The Ohio State University, 2001.
14. K. Ekinci, H. Keener, and D. Akbolat, *Effects of feedstock, airflow rate, and recirculation ratio on performance of composting systems with air recirculation*, Bioresource Technology **97** (2006), 922–932.
15. K. Ekinci, H. Keener, and D. Elwell, *Composting short paper fiber with broiler litter and additives: II. evaluation and optimization of decomposition rate versus mixing ratio*, Compost science & utilization **10** (2002), 16–28.
16. K. Ekinci, H. Keener, F. Michael, and D. Elwell, *Effects of temperature and initial moisture content on the composting rate of short paper fiber and broiler litter*, *Proceedings of ASAE Annual International Meeting*, California: ASAE, 2001, 1.
17. K. Ekinci, H. Keener, F. Michel, and D. Elwell, *Modeling composting rate as a function of temperature and initial moisture content*, Compost science & utilization **12** (2004), 356–364.
18. K. Ekinci, İ. Tosun, B. Bıtrak, B. Kumbul, F. Şevik, and K. Sülük, *Effects of initial c/n ratio on organic matter degradation of composting of rose oil processing solid wastes*, International Journal of Environmental Science and Technology **16** (2019), 5131–5140.
19. K. Ekinci, İ. Tosun, B. S. Kumbul, F. Şevik, K. Sülük, and N. B. Bıtrak, *Aeration requirement and energy consumption of reactor-composting of rose pomace influenced by c/n ratio*, Environmental Monitoring and Assessment **192** (2020), no. 9, 1–9.
20. K. Ekinci, I. Tosun, B. S. Kumbul, F. Şevik, K. Sülük, and N. B. Bıtrak, *Effect of initial c/n ratio on composting of two-phase olive mill pomace, dairy manure, and straw*, Environmental Progress & Sustainable Energy **40** (2021), no. 2, e13517.
21. K. Fukushima, C. Abbate, D. Tabuani, M. Gennari, and G. Camino, *Biodegradation of poly (lactic acid) and its nanocomposites*, Polymer Degradation and Stability **94** (2009), no. 10, 1646–1655.
22. M. Funabashi, F. Ninomiya, and M. Kunioka, *Biodegradability evaluation of polymers by iso 14855-2*, International journal of molecular sciences **10** (2009), no. 8, 3635–3654.
23. G. Gorrasi and R. Pantani, *Effect of pla grades and morphologies on hydrolytic degradation at composting temperature: Assessment of structural modification and kinetic parameters*, Polymer degradation and stability **98** (2013), no. 5, 1006–1014.
24. S. Grima, V. Bellon-Maurel, P. Feuilloley, and F. Silvestre, *Aerobic biodegradation of polymers in solid-state conditions: a review of environmental and physicochemical parameter settings in laboratory simulations*, Journal of Polymers and the Environment **8** (2000), 183–195.
25. J. Guckenheimer and P. Holmes, *Nonlinear oscillations, dynamical systems, and bifurcations of vector fields*, vol. 42, Springer Science & Business Media, 2013.
26. R. T. Haug, *The practical handbook of compost engineering*, Routledge, 2018.
27. S. Hemidat, M. Jaar, A. Nassour, and M. Nelles, *Monitoring of composting process parameters: a case study in jordan*, Waste and Biomass Valorization **9** (2018), 2257–2274.
28. M. W. Hirsch, S. Smale, and R. L. Devaney, *Differential equations, dynamical systems, and an introduction to chaos*, Academic press, 2012.
29. G. Huang, J. Wong, Q. Wu, and B. Nagar, *Effect of c/n on composting of pig manure with sawdust*, Waste management **24** (2004), no. 8, 805–813.
30. K. J. Jem and B. Tan, *The development and challenges of poly (lactic acid) and poly (glycolic acid)*, Advanced Industrial and Engineering Polymer Research **3** (2020), no. 2, 60–70.
31. N. Kabbashi, *Sewage sludge composting simulation as carbon/nitrogen concentration change*, Journal of Environmental Sciences **23** (2011), no. 11, 1925–1928.
32. N. Kabbashi, O. Suraj, M. Z. Alam, and M. Elwathig, *Kinetic study for compost production by isolated fungal strains*, Int J Waste Resour **4** (2014), no. 2.
33. J. Kaiser, *Modelling composting as a microbial ecosystem: a simulation approach*, Ecological modelling **91** (1996), no. 1-3, 25–37.
34. M. Karamanlioglu and G. D. Robson, *The influence of biotic and abiotic factors on the rate of degradation of poly (lactic) acid (pla) coupons buried in compost and soil*, Polymer Degradation and Stability **98** (2013), no. 10, 2063–2071.
35. H. Keener, K. Ekinci, and F. Michel, *Composting process optimization–using on/off controls*, Compost science & utilization **13** (2005), 288–299.
36. H. Keener, C. Marugg, H. Hoitink, and R. C. Hansen, *Design parameters for in-vessel poultry manure composting*, Paper-American Society of Agricultural Engineers (USA) (1991).
37. H. Keener, D. Elwell, K. Das, and R. Hansen, *Specifying design/operation of composting systems using pilot scale data*, Applied Engineering in Agriculture **13** (1997), no. 6, 767–772.
38. H. Keener, D. Elwell, F. Michel et al., *Effects of aeration strategies on the composting process: Part II. numerical modeling and simulation*, Transactions of the ASAE **48** (2005), 1203–1215.
39. H. M. Keener, R. C. Hansen, and C. Marugg, *Optimizing the efficiency of the composting process*, Ohio: The Ohio State University, 1992.

40. H. Khalil, *Nonlinear Systems*, Prentice Hall, 2002. URL https://books.google.cl/books?id=v_BjPQAACAAJ.
41. T. Leejarkpai, U. Suwanmanee, Y. Rudeekit, and T. Mungcharoen, *Biodegradable kinetics of plastics under controlled composting conditions*, Waste management **31** (2011), no. 6, 1153–1161.
42. L. Markus, *Ii. asymptotically autonomous differential systems*, Contributions to the Theory of Nonlinear Oscillations (AM-36) **3** (1953), 17.
43. C. Marugg, M. Grebus, R. Hansen, H. Keener, and H. Hoitink, *A kinetic model of the yard waste composting process*, Compost Science & Utilization **1** (1993), no. 1, 38–51.
44. M. A. M. Méndez, *La bifurcación triple cero en sistemas m-parametrizados*, Universidad de Sonora (2013).
45. S. Montoya, D. A. Ospina, and Ó. J. Sánchez, *Evaluation of the physical–chemical and microbiological characteristics of the phospho-compost produced under forced aeration system at the industrial scale*, Waste and Biomass Valorization **11** (2020), 5977–5990.
46. N. Mustafić, I. Petrić, and E. Karić, *Application of validated mathematical model of composting process for study the effect of air flow rate on process performance*, Journal of Engineering & Processing Management **9** (2017), 62–68.
47. V.-T. Nguyen et al., *Effects of c/n ratios and turning frequencies on the composting process of food waste and dry leaves*, Bioresource Technology Reports **11** (2020), 100527.
48. L. Perko, *Differential equations and dynamical systems*, vol. 7, Springer Science & Business Media, 2013.
49. I. Petric and V. Selimbašić, *Development and validation of mathematical model for aerobic composting process*, Chemical Engineering Journal **139** (2008), no. 2, 304–317.
50. V. Piemonte and F. Gironi, *Kinetics of hydrolytic degradation of pla*, Journal of Polymers and the Environment **21** (2013), 313–318.
51. F. Ruggero, R. Gori, and C. Lubello, *Methodologies to assess biodegradation of bioplastics during aerobic composting and anaerobic digestion: A review*, Waste Management & Research **37** (2019), no. 10, 959–975.
52. Z. Saadi, A. Rasmont, G. Cesar, H. Bewa, and L. Benguigui, *Fungal degradation of poly (l-lactide) in soil and in compost*, Journal of Polymers and the Environment **20** (2012), 273–282.
53. J. Sarasa, J. M. Gracia, and C. Javierre, *Study of the biodisintegration of a bioplastic material waste*, Bioresource technology **100** (2009), no. 15, 3764–3768.
54. T. Sokač et al., *An enhanced composting process with bioaugmentation: Mathematical modelling and process optimization*, Waste Management & Research **40** (2022), no. 6, 745–753.
55. J. SOTOMAYOR, *Generic bifurcations of dynamical systems ams (mos) 1970 subject classification: 58f99.*, M. PEIXOTO (ed.), *Dynamical Systems*, Academic Press, 1973. 561–582, . URL https://www.sciencedirect.com/science/article/pii/B9780125503501500473.
56. C. Soyöz, K. Ekinci, and Ş. Kilic, *Effects of recirculation of exhaust air in rotary drum composter on composting properties and energy consumption*, Waste and Biomass Valorization **12** (2021), 3645–3656.
57. N.-A. A. B. Taib et al., *A review on poly lactic acid (pla) as a biodegradable polymer*, Polymer Bulletin **80** (2023), no. 2, 1179–1213.
58. H. R. Thieme, *Asymptotically autonomous differential equations in the plane*, The Rocky Mountain Journal of Mathematics (1994), 351–380.
59. A. Thomson, G. Price, P. Arnold, M. Dixon, and T. Graham, *Review of the potential for recycling co2 from organic waste composting into plant production under controlled environment agriculture*, Journal of Cleaner Production **333** (2022), 130051.
60. M. M. Torki, S. Hassanajili, and M. M. Jalisi, *Design optimizations of pla stent structure by fem and investigating its function in a simulated plaque artery*, Mathematics and Computers in Simulation **169** (2020), 103–116.
61. E. C. Van Roijen and S. A. Miller, *A review of bioplastics at end-of-life: Linking experimental biodegradation studies and life cycle impact assessments*, Resources, Conservation and Recycling **181** (2022), 106236.
62. L. Wang, Y. Li, S. O. Prasher, B. Yan, Y. Ou, H. Cui, and Y. Cui, *Organic matter, a critical factor to immobilize phosphorus, copper, and zinc during composting under various initial c/n ratios*, Bioresource technology **289** (2019), 121745.
63. Q. Wang et al., *Improvement of pig manure compost lignocellulose degradation, organic matter humification and compost quality with medical stone*, Bioresource technology **243** (2017), 771–777.
64. O. Wilfred et al., *Biodegradation of polyactic acid and starch composites in compost and soil*, International Journal of Nano Research **1** (2018), no. 2, 1–11.
65. S. Wu et al., *Effects of c/n ratio and bulking agent on speciation of zn and cu and enzymatic activity during pig manure composting*, International Biodeterioration & Biodegradation **119** (2017), 429–436.

How to cite this article: Baldera-Moreno Y., Rojas-Palma A, and Andler R. A theoretical description of polylactic acid biodegradation in composting processes through mathematical modeling. *Math. Meth. Appl. Sci.* 2023;00(00):1–18.

APPENDIX

A NON-NEGATIVE CONE

Next, we will present definitions and properties necessary to prove the positivity of the system (29) [8].

Definition 2. An $n \times n$ real matrix A is a *graph Laplacian* if it has the following properties:

Property 1 (Pattern of signs). $A_{k,l} \geq 0$ for $k, l = 1, \ldots, n$, $k \neq l$, $A_{k,k} \leq 0$ for $k = 1, \ldots, n$.

Property 2 (Zero column sum). $\sum_{k=1}^{n} A_{k,l} = 0$, for $l = 1, \ldots, n$.

Definition 3. Let $A \subset \mathbb{R}^{n\times n}$, $A \neq \emptyset$, $\mathbb{R}_0^+ = \{x \in \mathbb{R} : x \geq 0\}$ is the set of non-negative real numbers. Then, A is a "non-negative cone" if $\mathbb{R}_0^+ \cdot A \subset A$.

Definition 4. Given two compatible matrices P and Q, we say that:

- $P \succ Q$ if $P_{i,j} > Q_{i,j}$ for all i, j and
- $P \succeq Q$ if $P_{i,j} \geq Q_{i,j}$ for all i, j.

Proposition 2 (Positivity). *If $X' = A(X) \cdot X$ with $X(0) = X_0 \succeq \mathbf{0}$, where $X \in \mathbb{R}^n$, and A is a graph Laplacian, then $X(t) \succeq \mathbf{0}$, for all $t \geq 0$*

B SOTOMAYOR'S THEOREM FOR M-PARAMETERIZED FAMILIES

The following theorem will allow us to show under what conditions a bifurcation occurs at a non-hyperbolic equilibrium point of codimension one of an m-parametric system [2, 44].

Theorem 4. *Consider the parameterized system*

$$x' = F(x, k) \tag{B1}$$

with $x \in \mathbb{R}^n$ and $k \in \mathbb{R}^m$. Suppose that there is (x_0, k_0) such that

H1) $F(x_0, k_0) = 0$,
H2) $\sigma(A) = \{\lambda_1 = 0, Re(\lambda_j) \neq 0, for\, j = 2, 3, \ldots, m\}$.

Let v_0 and w_0 be the right and left eigenvectors respectively of $A = DF(x_0, k_0)$ corresponding to the eigenvalue $\lambda_1 = 0$. Then,

(1) If

$$a = w_0^T F_k(x_0, k_0) \neq 0, \tag{B2}$$
$$b = (w_0^T D^2 F(x_0, k_0))(v_0, v_0) \neq 0. \tag{B3}$$

Then, the System (B1) *experiences a saddle-node bifurcation at the equilibrium point $x = x_0$ when the parameter k passes through the bifurcation value $k = k_0$.*

(2) If

$$a = w_0^T F_k(x_0, k_0) = 0, \tag{B4}$$
$$b = (w_0^T D^2 F(x_0, k_0))(v_0, v_0) \neq 0, \tag{B5}$$
$$c = -(w_0^T D^2 F(x_0, k_0))(v_0, P_0) J_s^{-1} Q_0 F_k(x_0, k_0) + v_0^T (w_0^T F_{kx}(x_0, k_0))^T \neq 0. \tag{B6}$$

Then, the System (B1) *experiences a transcritical bifurcation at the equilibrium point $x = x_0$ when the parameter k passes through the bifurcation value $k = k_0$.*

(3) If

$$a = w_0^T F_k(x_0, k_0) = 0, \tag{B7}$$
$$b = (w_0^T D^2 F(x_0, k_0))(v_0, v_0) = 0, \tag{B8}$$
$$c = -(w_0^T D^2 F(x_0, k_0))(v_0, P_0) J_s^{-1} Q_0 F_k(x_0, k_0) + v_0^T (w_0^T F_{kx}(x_0, k_0))^T \neq 0, \tag{B9}$$
$$d = \frac{1}{6}(w_0^T D^3 F(x_0, k_0))(v_0, v_0, v_0) - \frac{1}{2}(w_0^T D^2 F(x_0, k_0))(v_0, P_0) J_s^{-1} (Q_0 D^2 F(x_0, k_0))(v_0, v_0) \neq 0. \tag{B10}$$

Then, the System (B1) *experiences a pitchfork bifurcation at the equilibrium point $x = x_0$ when the parameter k passes through the bifurcation value $k = k_0$.*

The proof for the uniparametric case, i.e., when $k = 1$, can be found in [48, 55, 25], and the generalization of the k-parametric case [2, 44].